Hybrid Spoof Surface Plasmon Polariton and Substrate Integrated Waveguide Transmission Line and Its Application in Filter

Dong-Fang Guan, Peng You, Qingfeng Zhang, *Senior Member, IEEE*, Ke Xiao, and Shao-Wei Yong

***Abstract*— In this paper, spoof surface plasmon polariton (SPP) is integrated in the closed substrate integrated waveguide (SIW) structure and a novel hybrid SIW-SPP guided-wave transmission line (TL) is proposed. In this design, the surface wave mode of SPP can be excited and transmitted inside the closed structure of SIW. The dispersion property of the proposed SIW-SPP hybrid structure indicates that it has both slow wave feature of SPP and fast-wave feature of SIW. With the low-pass feature of SSP and the high-pass feature of SIW, the proposed hybrid SIW-SPP TL becomes a bandpass filter (BPF) naturally. The concept of integrating SPP and SIW opens a new way to develop novel wideband BPFs. A broadband filter is fabricated to verify the theory and the measured passband is from 16.1 to 25.4 GHz with a relative bandwidth of 43.8%. The filter bandwidth can be easily controlled by tuning parameters, thus the proposed structure is attractive and useful for the design of various BPFs.**

***Index Terms*— Bandpass filter (BPF), substrate integrated waveguide (SIW), surface plasmon polariton (SPP), wideband.**

I. Introduction

SURFACE plasmon polaritons (SPPs) are a special kind of surface electromagnetic waves propagating along the surface of a conductor at optical frequencies [1], [2]. With the advantage of confining light in subwavelength region, SPPs have potential applications in the design of high-density integrated optical components and circuits. The SPPs were originally used at optical frequencies until Pendry *et al.* [3] and Garcia-Vidal [4] developed a new structure to mimic the characteristics of SPPs at microwave and terahertz bands in 2004. Using periodic subwavelength holes on the metal surface, the proposed spoof SPPs are similar in many aspects to optical SPPs. After that, much effort has been made to design spoof SPPs at low frequencies.

In previous works, spoof SPPs were designed mainly using metal materials decorated with subwavelength grooves or holes [3]–[10]. In [5], a periodically corrugated conducting coaxial waveguide was developed for propagation of localized spoof SPPs. 2-D through or blind holes arrays were perforated on metal substrates to realize spoof SPPs waveguide in [6] and [7]. However, all of the aforementioned spoof SPPs are based on 3-D metallic structures, which have a major limitation associated with their design complexity and high cost. Besides, these structures are difficult to be integrated with planar circuits. Recently, Shen *et al.* [11] introduced a novel planar strip transmission line (TL) with the subwavelength corrugated structure, which can support and propagate surface plasmon modes on electrically ultrathin and flexible films. This opens a new way to develop planar spoof SPPs [12]–[24]. To make the use of spoof SPPs in microwave circuits, efficient conversion from SPPs to traditional planar TLs is essential. Transition between SPP and coplanar waveguide (CPW) was exploited in [12] and [13]. In another study, SPP TL coupled to microstrip TL was designed and fabricated [14]. Due to the advantages of high-field confinement, flexible planar structure, and slow wave characteristic, spoof SPP has inspired many research works in the design of microwave and millimeter-wave devices, including frequency splitters [15], [16], filters [17]–[21], and antennas [22]–[24]. Nevertheless, the proposed planar spoof SPPs are constructed by corrugated strip lines and are all open structures. Thus, the radiation loss and the mutual coupling (MC) with other TLs or devices are inevitable.

To overcome the disadvantages of 3-D metallic TLs and planar open TLs, substrate integrated waveguide (SIW) was proposed [25], [26]. Through digging two rows of metallic via holes on printed circuit board (PCB) substrate, SIW has the similar performance to metallic waveguide, i.e., low-insertion loss, low interference, and low radiation. Besides, it has the merits of low profile and integrability with other planar circuits. There have been attempts to integrate SIW with other planar TLs to build up novel hybrid guided-wave structures [28]–[31]. For example, an SIW-CPW hybrid guided-wave TL was developed in [30], which has the advantages of both SIW and CPW. To the best of our knowledge, the spoof SPPs with metallic block and planar strip line structures have been investigated sufficiently, but the spoof SPPs based on SIW structure have not been reported so far. With the wide application of SIW and the rapid development of SPPs, it is attractive to construct SPP in SIW structure and realize conversion from SPP to SIW directly.

Manuscript received February 9, 2017; revised May 5, 2017; accepted July 1, 2017. Date of publication July 24, 2017; date of current version December 12, 2017. This work was supported in part by the Natural Science Foundation of Hunan Province, China, under Grant 2017JJ3364, and in part by the National Natural Science Foundation of China under Grant 61601487, and Guangdong NSF for DYS (2015A030306032). *(Corresponding authors: Peng You; Qingfeng Zhang.)*

D.-F. Guan, P. You, K. Xiao, and S.-W. Yong are with the College of Electronic Science and Engineering, National University of Defense Technology, Changsha 410073, China (e-mail: gdfguandongfang@163.com; ypnudt@126.com).

Q. Zhang is with the Department of Electronics and Electrical Engineering, Southern University of Science and Technology, Shenzhen 518055, China (e-mail: zhang.qf@sustc.edu.cn).

Color versions of one or more of the figures in this paper are available online at http://ieeexplore.ieee.org.

Digital Object Identifier 10.1109/TMTT.2017.2727486

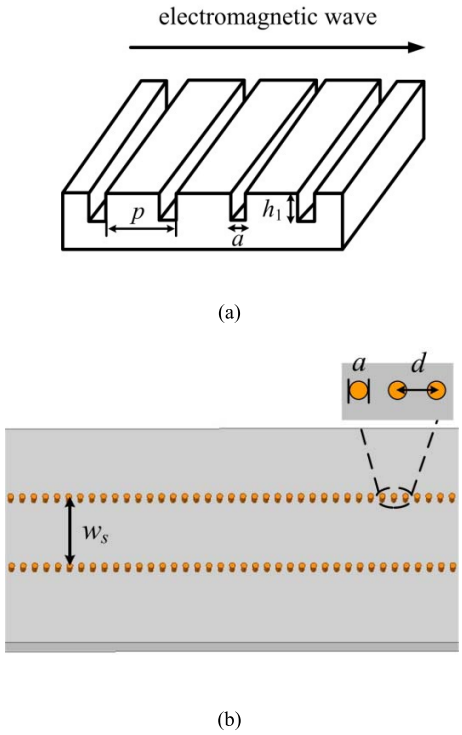

Fig. 1. Configurations of SPP and SIW. (a) SPP TL with corrugated metallic structure. (b) SIW TL.

In this paper, we propose a hybrid SIW-SPP transmission structure, in which SPP is designed inside the SIW TL through employing arrays of transverse metallic blind holes. In this design, we first develop a closed SPP TL in planar structure and realize integration of SPP and SIW. The proposed hybrid structure has the features of both SIW and SPP. SIW is a fast-wave waveguide and has a lower cutoff frequency, while SPP has slow wave and low-pass features. It is a novel concept to design bandpass filter (BPF) based on cutoff frequencies of SIW and SPP. Besides, the bandwidth of this filter can be easily adjusted by tuning the parameters of SIW-SPP. The paper is organized as follows. The configuration and characteristics analysis of SIW-SPP hybrid TL are presented in Section II. Section III describes the procedure of designing a wideband filter based on this hybrid SIW-SPP structure, followed by an experimental validation. Finally, the paper is summarized in Section IV.

II. Principle of Hybrid SIW-SPP Structure

A. Dispersion Analysis of SPP and SIW

Fig. 1(a) and (b) is the typical configurations of SPP and SIW TLs. As shown in Fig. 1(a), the grooves are corrugated in a perfect conductor to construct a spoof SPP structure. The width and depth of grooves are a and h_1, respectively, and the period of the SPP element is p. It has been proven that such periodic metallic grooves can support and propagate a surface plasmon mode at microwave frequencies, when a and p are much less than the wavelength at the operational frequency. The dispersion relation of such SPP is [5]

$$\beta = k_0\sqrt{1+\frac{a^2}{p^2}\tan^2(k_0h_1)} \tag{1}$$

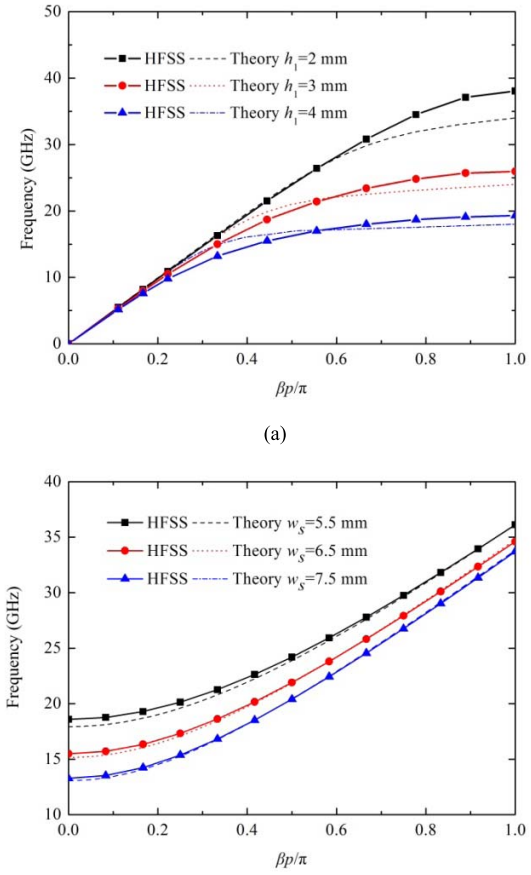

Fig. 2. Dispersion diagrams. (a) SPP. (b) SIW.

where β is the propagation constant of the SPP mode and $k_0 = \omega/c$. The dispersion curve of this SPP is also analyzed using Ansoft HFSS in comparison with the theoretical data, as shown in Fig. 2(a). It can be observed that the dispersion curves deviate gradually to the slow wave region as β increases. Besides, the curves exhibit decreased upper cutoff frequencies as the groove depth h_1 increases.

As shown in Fig. 1(b), SIW is composed of two rows metallic via holes on PCB, where a is the diameter of the metallic via holes and d is the hole spacing. When a is chosen to be smaller than a tenth of the wavelength at the maximum operational frequency and p is smaller than twice of a, SIW is equivalent to a metallic rectangular waveguide. The fundamental mode in SIW is TE_{10} mode and the dispersion relationship is [27]

$$\beta \approx \sqrt{\varepsilon_r\mu_r k_0^2 - \left(\frac{\pi}{w_s}\right)^2} \tag{2}$$

where β is the propagation constant of TE_{10} mode, w_s is the width of SIW, ε_r and μ_r are the relative permittivity and permeability. The simulated and theoretical dispersion curves of SIW are depicted in Fig. 2(b). It can be observed that the curves are in the fast-wave region and there exists a lower cutoff frequency for SIW. The lower cutoff frequency of SIW TL is inversely proportional to the width w_s.

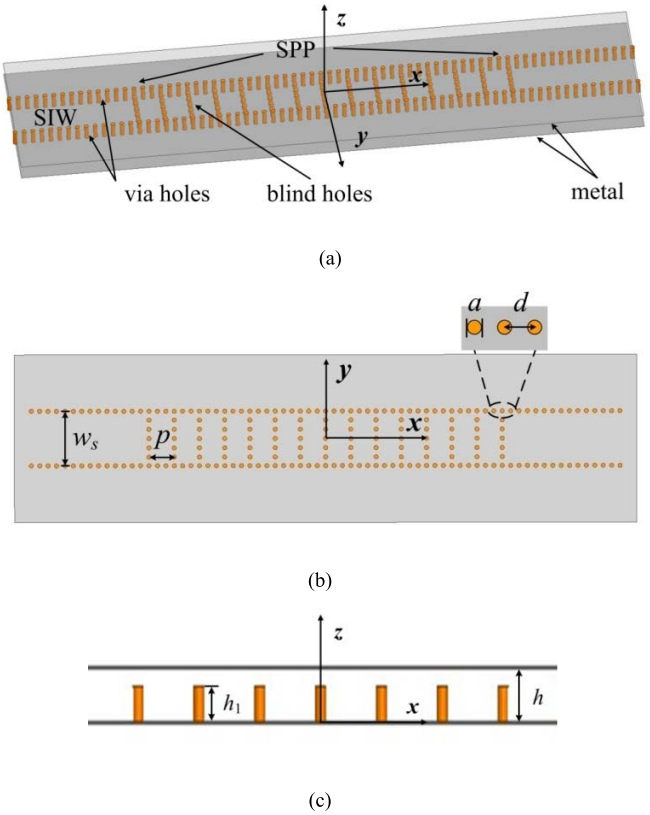

Fig. 3. Configuration of the proposed hybrid SIW-SPP structure. (a) Perspective view. (b) Top view. (c) Profile view.

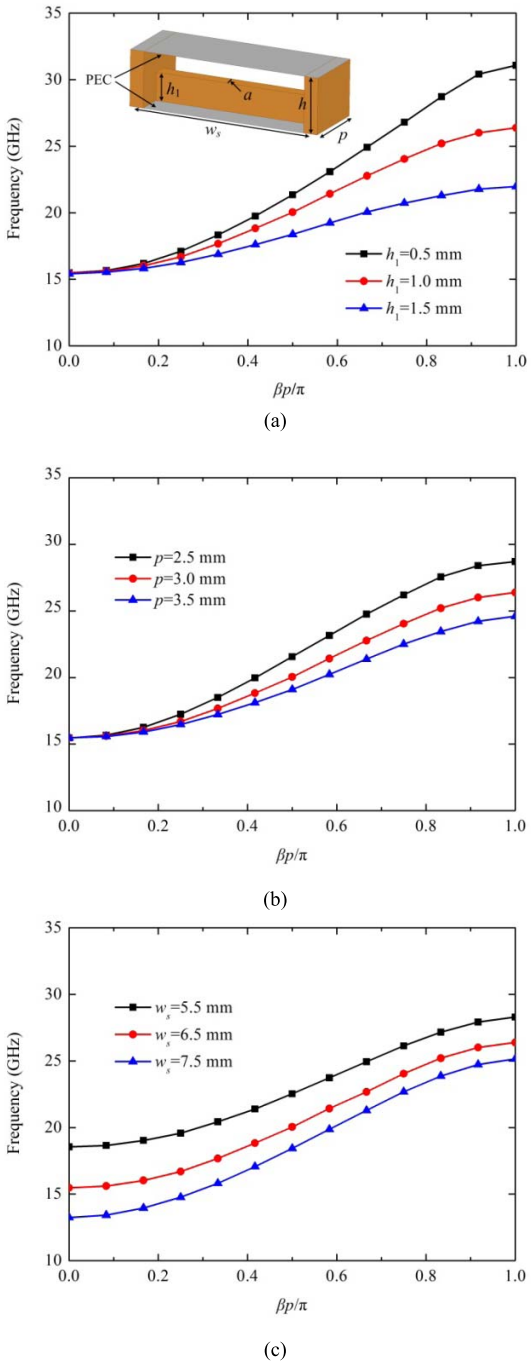

Fig. 4. Simulated dispersion diagrams of the proposed hybrid SIW-SPP structure. (a) With different heights of SPP h_1. (b) With different periods of SPP p. (c) With different widths of SIW w_s.

B. Dispersion Analysis of Hybrid SIW-SPP

In this paper, we present a hybrid SIW-SPP TL, as shown in Fig. 3, in which the spoof SPP is designed in SIW structure for the first time. It is designed on a single-layer F4BM-2 PCB with thickness $h = 2$ mm, relative dielectric constant $\varepsilon_r = 2.65$, and loss tangent $\tan\delta = 0.001$. For traditional 3-D metallic spoof SPPs or planar strip line spoof SPPs, the surface wave is transmitted in the open or half open space. In our design, SPP is designed inside SIW by employing arrays of transverse metallic blind holes as equivalent corrugated grooves, and the surface wave mode of SPP is propagated totally inside the closed SIW structure. Therefore, the radiation loss is small and the transmission efficiency can be improved.

Moreover, the proposed hybrid SIW-SPP structure has the characteristics of both SIW and SPP. The periodic element of the proposed SIW-SPP is simulated with the eigen mode analysis of Ansoft HFSS. The simulated model and parameters of the SIW-SPP element are depicted in Fig. 4(a). To reduce the simulation time, the metallic via holes of SIW and blind holes of SPP are replaced by metallic walls [brown part in Fig. 4(a)]. The dispersion diagrams with different parameters are presented in Fig. 4. Compared with the dispersion curves of SPP and SIW in Fig. 2, the dispersion curves of the proposed hybrid SIW-SPP have both lower and upper cutoff frequencies. In the left part of Fig. 4, the curves are concave and the fast-wave feature of SIW is obvious. As β increases, the curves become convex gradually and the slow wave feature of SPP is emerged in the right part. Fig. 4(a) shows the influence of metallic blind holes height h_1 (the depth of grooves) on the dispersion curves. As h_1 increases, the upper cutoff frequency of SPP is reduced while the lower cutoff frequency remains the same. It meets the theoretical dispersion relations of SPP and SIW mentioned above. As shown in Fig. 4(b), the period of SPP element p also has influence on the dispersion characteristic of SPP. When p becomes longer, the upper cutoff frequency is smaller. Fig. 4(c) gives the simulated dispersion diagrams for different SIW

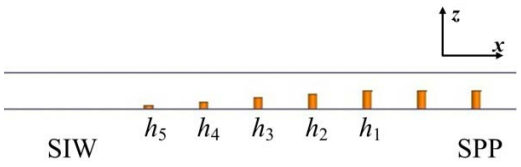

Fig. 5. Configuration of conversion between SIW and SPP.

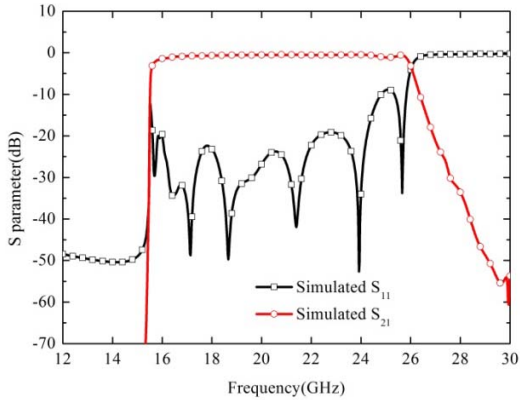

Fig. 6. Simulated reflection coefficient (S_{11}) and transmission coefficient (S_{21}) of the proposed hybrid SIW-SPP structure.

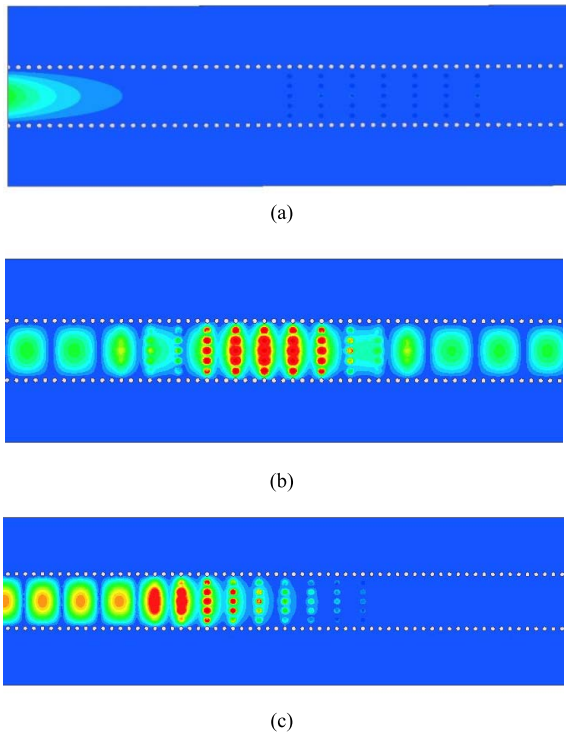

Fig. 7. Simulated electric-field distributions of proposed hybrid SIW-SPP structure. (a) At the lower frequency stopband. (b) At the passband. (c) At the upper frequency stopband.

widths w_s. It can be observed that the lower cutoff frequencies for different w_s are similar to those of SIW in Fig. 2(b). Besides, the upper cutoff frequency is also changed by tuning the width of SIW, since w_s is also the thickness of SPP and hence has influence on the dispersion feature of SPP [11].

C. Transmission Analysis of Hybrid SIW-SPP

The simulated dispersion curves indicate that the hybrid SIW-SPP element has the dispersion features of both SIW and SPP. For applying such spoof SPP structure to microwave and millimeter-wave devices, efficient conversion from SPP to planar circuits are needed. Unlike complicated conversion with microstrip line or CPW for traditional spoof SPPs, the proposed hybrid SIW-SPP structure can be converted to SIW TL directly. Fig. 5 shows the transition from SIW to SPP. Four rows of transverse metallic blind holes with tapered heights are placed at the end of SPP to reduce the impedance mismatch between the two structures, leading to a smooth conversion from TE_{10} mode of SIW to TM mode of SPP. In our design, the tapered heights are set as

$$h_i = (1.2 - 0.2 \cdot i) \cdot h_1, \quad i = 2, 3, 4, 5. \tag{3}$$

Fig. 6 is the simulated reflection coefficients (S_{11}) and transmission coefficients (S_{21}) of the proposed hybrid SIW-SPP TL. The center operating frequency of the TL is set at 20 GHz. The length of SPP excluding the transition part is 5λ, where λ is the space wavelength at the center frequency. It can be seen that the signal can efficiently transmit through such hybrid TL within the lower and upper cutoff frequencies in accordance with the dispersion curves of Fig. 4. Within the range of 16.3–25.8 GHz, the reflection coefficient (S_{11}) is lower than -9 dB and the transmission coefficient (S_{21}) is higher than -1.1 dB. The simulated electric-field distributions of the proposed hybrid SIW-SPP structure are shown in Fig. 7. As shown in Fig. 7(a), the signal cannot propagate through SIW when its frequency is smaller than the lower cutoff frequency of SIW. On the other hand, the signal will disappear gradually and cannot propagate through SPP when its frequency is higher than the upper cutoff frequency of SPP, as shown in Fig. 7(c). Within the passband, the signal can get through the hybrid SIW-SSP TL and realize efficient mode conversion, as shown in Fig. 7(b).

The insertion loss of the proposed TL includes two parts, the conversion loss and the transmission loss. The conversion loss caused by the transition part is constant while the transmission loss is related to the length of SPP elements. In order to analyze the insertion loss, transmission coefficients (S_{21}) with different TL lengths are simulated. The lengths of SPP TL excluding the transition part are set as 0, 5λ, 10λ, and 20λ, respectively. As shown in Fig. 8, the corresponding losses at 20 GHz are 0.12, 0.53, 0.98, and 2.05 dB, respectively. When the length of SPP elements is zero, the insertion loss is only 0.12 dB. It means that the conversion loss is less than 0.12 dB. By comparing the other curves in Fig. 8, one finds that the transmission loss increases by approximately 1 dB as the length increases by 10λ. Two SIW-SPP TLs with length of 5λ are placed side-by-side with the spacing of d_{mc} to study the MC effect. The simulated result is shown in Fig. 9. Since the electromagnetic wave is almost restricted inside the SIW, the MC between SIW-SPP TLs is very low compared to that of strip SPP TL in [13].

In summary, the hybrid SIW-SPP TL has some advantages compared to other planar SPP TLs [12]–[14]. First, the

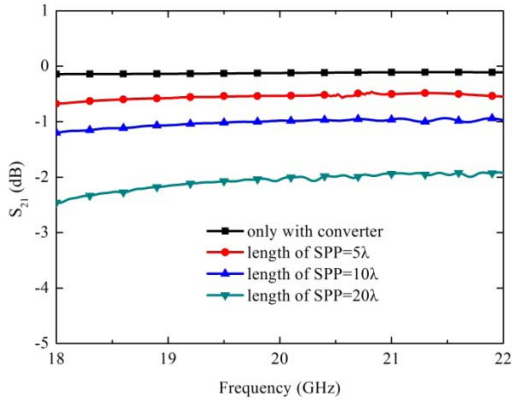

Fig. 8. Simulated transmission coefficients (S_{21}) with different SIW-SPP TL lengths.

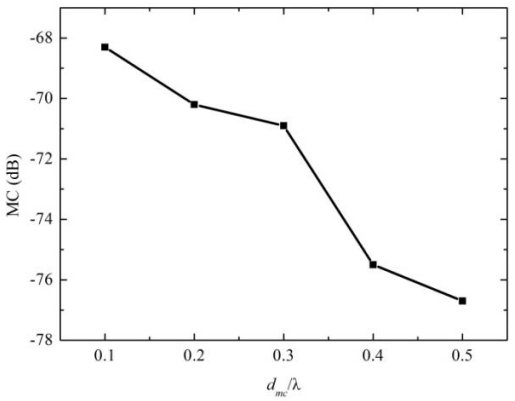

Fig. 9. Simulated MC effect of SIW-SPP TLs.

conversion between SIW and SPP is simple and the conversion loss is very small. Second, the radiation loss and MC are negligible due to its close structure. Third, the transmission performance will not get bad when the field confinement ability of SPP becomes weak at the lower frequencies, contrary to other planar SPP TLs [12].

III. Hybrid SIW-SPP Filter

Below the upper cutoff frequency, SPP TL is a low-pass filter. This opens a new way to develop novel filters [17]–[21]. In [21], SPP and SIW TLs were cascaded to design a BPF with controllable bandwidth. However, the two TLs are independent and have to be connected through microstrip line for modes conversion. Thus the filter has a large size and the design is complicated. According to the analysis of the proposed hybrid SIW-SPP structure above, it has both upper and lower cutoff frequencies and hence exhibits BPF feature. Moreover, its structure is compact compared with that of [21], due to the integration of SIW and SPP.

The passband of the proposed filter is determined by the cutoff frequencies, which can be tuned independently. The simulated transmission coefficients (S_{21}) of the filter with different parameters are presented in Fig. 10. It can be seen that the lower cutoff frequency of the filter is only determined by the width of SIW. The upper cutoff frequency is mainly affected by the groove depth of SPP and SIW

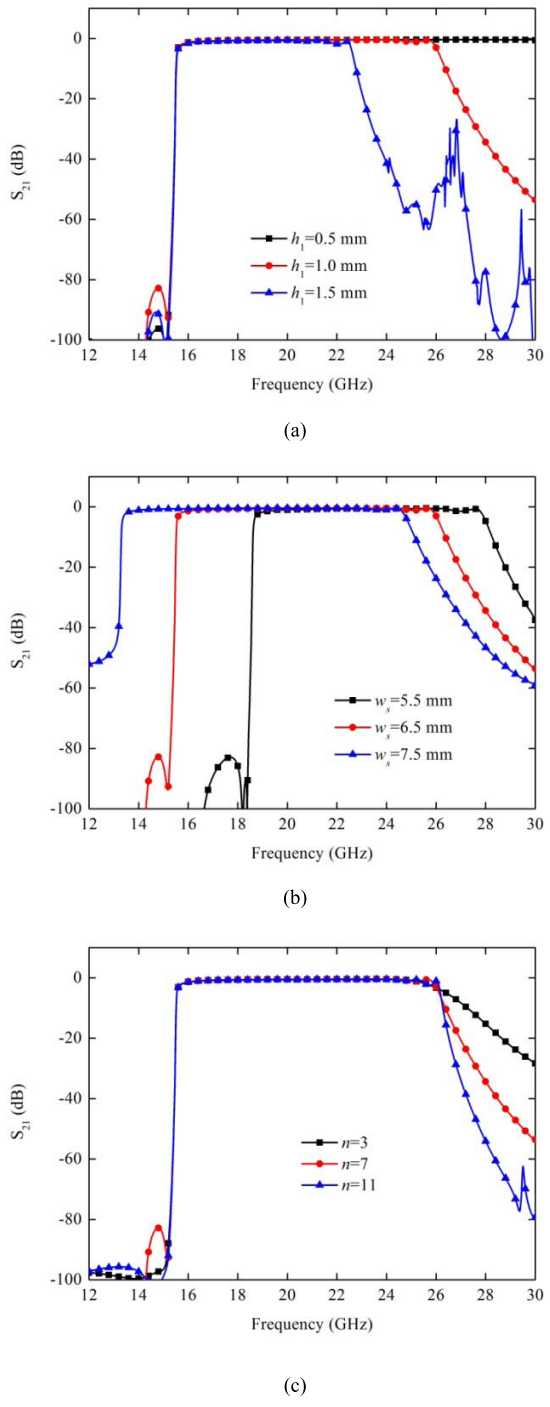

Fig. 10. Simulated transmission coefficients (S_{21}) of the filter. (a) With different groove depths h_1. (b) With different SIW widths w_s. (c) With different numbers of SPP elements n.

width as well. Therefore, the lower cutoff frequency should be determined first by tuning parameter w_s and then the upper cutoff frequency can be set by tuning parameter h_1. In this design procedure, the cutoff frequencies of passband can be set independently and the filter bandwidth can be easily adjusted. Fig. 10(c) depicts the influence of parameter n on the filter performance, where n is the number of SPP elements. It can be seen that the out of band rejection is higher as the number of SPP element increases.

TABLE I
DIMENSION VALUES OF THE FILTER

p	a	w_s	d	n
3 mm	0.5 mm	6.5 mm	1 mm	5
h_1	h_2	h_3	h_4	h_5
1 mm	0.8 mm	0.6 mm	0.4 mm	0.2 mm

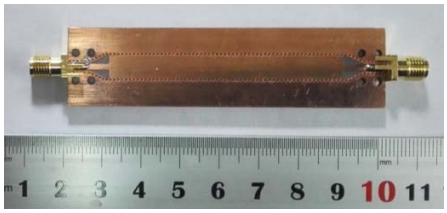

(a)

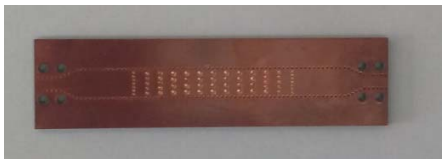

(b)

Fig. 11. Photograph of the fabricated filter. (a) Obverse side. (b) Reverse side.

TABLE II
PERFORMANCE COMPARISON OF DIFFERENT SIW FILTERS

	f (GHz)	BW (%)	Insertion loss (dB)	Return loss (dB)	Rejection (dB)	Length (λ)	Type
[32]	12.25	61.5	1.55	>10	40	2.6	SIW with periodic CPW
[33]	7.25	28	1.5	>17	25	1.85	Zigzag SIW structure
[34]	8.5	42	1.1	>11	20	1.25	SIW with U slot
[35]	6.43	89.6	1.55	>15	20	0.99	Ridge half-mode SIW
Our work	21	43.8	1.02	>10	25	3.15	Hybrid SIW and SPP

To validate the proposed structure and analysis, a broadband filter is fabricated and measured. After optimization with Ansoft HFSS, the geometry parameters of the filter are listed in Table I. A prototype is fabricated on the single-layer F4BM-2 substrate, and the photograph of the filter prototype is shown in Fig. 11. In order to measure the proposed filter, 50 Ω CPW lines are added to both ends of SIW. By changing the gap between strip and ground, the impedance of CPW can be tuned. Thus, tapered gaps are used for the transition from SIW to CPW. As shown in Fig. 11(b), the transverse blind holes are designed and metallized on the reverse side of the substrate. Due to the fabrication limit, the height and diameter of the holes must be identical. The SPP heights cannot be changed, thus the diameter of the blind holes have to be adjusted.

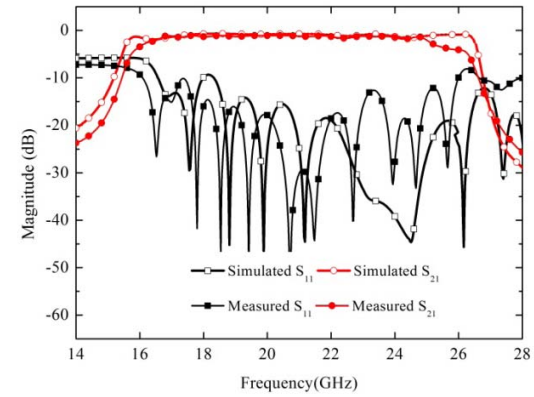

(a)

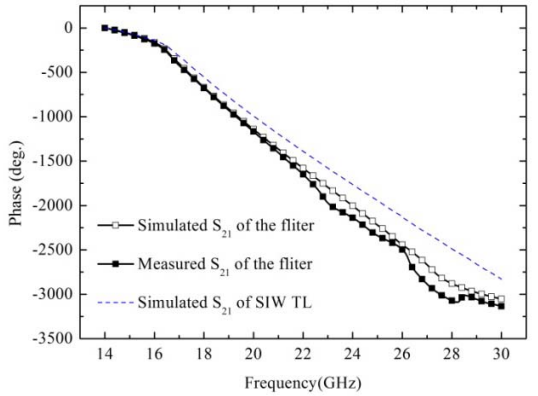

(b)

Fig. 12. Measured and simulated reflection coefficients (S_{11}) and transmission coefficients (S_{21}) of the filter. (a) Magnitude. (b) Phase.

Fig. 12(a) presents the measured and simulated magnitude curves of the reflection coefficients (S_{11}) and transmission coefficients (S_{21}). It can be seen that the adjustment of blind hole diameter has no influence on the filter performance. The trend of the measured curves agrees well with the simulated ones. The simulated 3-dB bandwidth is from 15.5 to 26.5 GHz and the measured one is from 16.1 to 25.4GHz. Within the whole frequency range, the measured S_{11} magnitude is below -10 dB. The insertion losses of the simulated and measured S_{21} are 0.74 and 1.02 dB at the center frequency of 21 GHz. Besides, the simulated S_{21} of Fig. 12(a) exhibits less selective response at the lower cutoff frequency than that of Fig. 6, which is possibly caused by the additional CPW-to-SIW transition in the experimental measurement. It is supposed that the performance of the proposed filter is much better if only SIW-SSP part is considered. The simulated and measured phase curves of S_{21} are shown in Fig. 12(b) in comparison with that of a pure SIW TL. Note that the phase velocity of the proposed SIW-SPP is slower than that of a pure SIW.

Table II compares the proposed filter with some representative wideband SIW filters. Note that, the bandwidth of the proposed filter is not the widest. However, since the upper and lower cutoff frequencies can be adjusted independently, the proposed filter potentially can further increase

the bandwidth. Furthermore, the propsoed filter is actually a simple TL, thus the insertion loss is the lowest. In conclusion, the operation mechanism of the proposed hybrid SIW-SPP filter is different from traditional ones and it is an attractive attempt to design novel filters using hybrid SIW-SPP TLs.

IV. Conclusion

In this paper, a hybrid SIW-SPP transmission structure has been proposed. The SPP is integrated with an SIW structure by employing arrays of transverse metallic blind holes in planar configurations. The dispersion and transmission characteristics of the proposed SIW-SPP TL were simulated and analyzed. It reveals that the hybrid SIW-SPP structure has the dispersion characteristics of both SPP and SIW. Besides, its transmission performance is excellent due to its closed structure. The concept of integrating SPP and SIW opens a new way to develop novel wideband BPFs. To test and verify the theory, a filter sample was fabricated, and the measured 3-dB bandwidth is 43.8%. Since the filter bandwidth can be controlled by tuning the parameters of SIW and SPP, the proposed design is attractive and can be used to develop ultra wideband BPFs.

References

[1] H. Raether, *Surface Plasmons on Smooth and Rough Surfaces and on Gratings* (Springer Tracts in Modern Physics), vol. 111. New York, NY, USA: Springer, 1988.

[2] W. L. Barnes, A. Dereux, and T. W. Ebbesen, "Surface plasmon subwavelength optics," *Nature*, vol. 424, no. 6950, pp. 824–830, 2003.

[3] J. B. Pendry, L. Martín-Moreno, and F. J. Garcia-Vidal, "Mimicking surface plasmons with structured surfaces," *Science*, vol. 305, pp. 847–848, Aug. 2004.

[4] F. Garcia-Vidal, L. Martín-Moreno, and J. B. Pendry, "Surfaces with holes in them: New plasmonic metamaterials," *Opt. A, Pure Appl. Opt.*, vol. 7, no. 2, p. S97, 2005.

[5] N. Talebi and M. Shahabadi, "Spoof surface plasmons propagating along a periodically corrugated coaxial waveguide," *J. Phys. D, Appl. Phys.*, vol. 43, no. 13, p. 135302, Mar. 2010.

[6] W. Zhu, A. Agrawal, and A. Nahata, "Planar plasmonic terahertz guided-wave devices," *Opt. Exp.*, vol. 16, no. 9, pp. 6216–6226, Apr. 2008.

[7] W. Zhu, A. Agrawal, A. Cui, G. Kumar, and A. Nahata, "Engineering the propagation properties of planar plasmonic terahertz waveguides," *IEEE J. Sel. Topics Quantum Electron.*, vol. 17, no. 1, pp. 146–153, Feb./Jan. 2011.

[8] J. J. Wu, D. J. Hou, T. J. Yang, I. J. Hsieh, Y. H. Kao, and H. E. Lin, "Bandpass filter based on low frequency spoof surface plasmon polaritons," *Electron. Lett.*, vol. 48, no. 5, pp. 269–270, 2012.

[9] H. Yi, S.-W. Qu, and X. Bai, "Antenna array excited by spoof planar plasmonic waveguide," *IEEE Antennas Wireless Propag. Lett.*, vol. 13, pp. 1227–1230, 2014.

[10] H. Yi, C. Zheng, and S.-W. Qu, "Spoof plasmonic waveguide-fed 2-D antenna array with improved efficiency," *IEEE Antennas Wireless Propag. Lett.*, vol. 16, pp. 377–380, 2017.

[11] X. Shen, T. J. Cui, D. Martin-Cano, and F. J. Garcia-Vidal, "Conformal surface plasmons propagating on ultrathin and flexible films," *Proc. Nat. Acad. Sci. USA*, vol. 110, no. 1, pp. 40–45, 2013.

[12] H. F. Ma, X. Shen, Q. Cheng, W. X. Jiang, and T. J. Cui, "Broadband and high-efficiency conversion from guided waves to spoof surface plasmon polaritons," *Laser Photon. Rev.*, vol. 8, no. 1, pp. 146–151, 2014.

[13] A. Kianinejad, Z. N. Chen, and C.-W. Qiu, "Low-loss spoof surface plasmon slow-wave transmission lines with compact transition and high isolation," *IEEE Trans. Microw. Theory Techn.*, vol. 64, no. 10, pp. 3078–3086, Oct. 2016.

[14] A. Kianinejad, Z. N. Chen, and C.-W. Qiu, "Design and modeling of spoof surface plasmon modes-based microwave slow-wave transmission line," *IEEE Trans. Microw. Theory Techn.*, vol. 63, no. 6, pp. 1817–1825, Jun. 2015.

[15] X. Shen, G. Moreno, A. Chahadih, T. Akalin, and T. J. Cui, "Spoof surface plasmonic devices and circuits in THz frequency," in *Proc. IRMMW-THz*, Tucson, AZ, USA, Sep. 2014, p. 1.

[16] J. Shibayama, J. Yamauchi, and H. Nakano, "Metal disc-type splitter with radially placed gratings for terahertz surface waves," *Electron. Lett.*, vol. 51, no. 4, pp. 352–353, 2015.

[17] X. Gao, L. Zhou, Z. Liao, H. F. Ma, and T. J. Cui, "An ultra-wideband surface plasmonic filter in microwave frequency," *Appl. Phys. Lett.*, vol. 104, no. 19, p. 191603, 2014.

[18] B. C. Pan, Z. Liao, J. Zhao, and T. J. Cui, "Controlling rejections of spoof surface plasmon polaritons using metamaterial particles," *Opt. Exp.*, vol. 22, no. 11, pp. 13940–13950, 2014.

[19] J. Y. Yin, J. Ren, H. C. Zhang, B. C. Pan, and T. J. Cui, "Broadband frequency-selective spoof surface plasmon polaritons on ultrathin metallic structure," *Sci. Rep.*, vol. 5, Feb. 2015, Art. no. 8165.

[20] L. Liu, Z. Li, B. Xu, P. Ning, C. Chen, and C. Gu, "An ultra-wideband low-pass plasmonic filter based on spoof surface plasmon polaritons," in *Proc. Asia–Pacific Microw. Conf. (APMC)*, Dec. 2015, pp. 1–3.

[21] Q. Zhang, H. C. Zhang, H. Wu, and T. J. Cui, "A hybrid circuit for spoof surface plasmons and spatial waveguide modes to reach controllable band-pass filters," *Sci. Rep.*, vol. 5, Nov. 2015, Art. no. 16531.

[22] J. Y. Yin *et al.*, "Frequency-controlled broad-angle beam scanning of patch array fed by spoof surface plasmon polaritons," *IEEE Trans. Antennas Propag.*, vol. 64, no. 12, pp. 5181–5189, Dec. 2016.

[23] A. Kianinejad, Z. N. Chen, and C.-W. Qiu, "A single-layered spoof-plasmon-mode leaky wave antenna with consistent gain," *IEEE Trans. Antennas Propag.*, vol. 65, no. 2, pp. 681–687, Feb. 2017.

[24] A. Kianinejad, Z. N. Chen, L. Zhang, W. Liu, and C.-W. Qiu, "Spoof plasmon-based slow-wave excitation of dielectric resonator antennas," *IEEE Trans. Antennas Propag.*, vol. 64, no. 6, pp. 2094–2099, Jun. 2016.

[25] W. Hong *et al.*, "SIW-like guided wave structures and applications," *IEICE Trans. Electron.*, vol. E92-C, no. 9, pp. 1111–1123, Sep. 2009.

[26] K. Wu, D. Deslandes, and Y. Cassivi, "The substrate integrated circuits—A new concept for high-frequency electronics and optoelectronics," in *Proc. 6th Int. Conf. Telecommun. Modern Satellite, Cable Broadcast. Service (TELSIKS)*, vol. 1. Oct. 2003, pp. P-3–P-5.

[27] M. Salehi and E. Mehrshahi, "A closed-form formula for dispersion characteristics of fundamental SIW mode," *IEEE Microw. Wireless Compon. Lett.*, vol. 21, no. 1, pp. 4–6, Jan. 2011.

[28] D.-F. Guan, Z.-P. Qian, Y.-S. Zhang, Y. Cai, and W.-Q. Cao, "A forward narrow-wall double-slot 3 dB coupler based on hybrid HSIW/GCPW guided-wave structure," *J. Electromagn. Waves Appl.*, vol. 28, no. 3, pp. 289–294, Mar. 2014.

[29] D.-F. Guan, Z.-P. Qian, Y.-S. Zhang, and Y. Cai, "A hybrid SIW and GCPW guided-wave structure coupler," *IEEE Microw. Wireless Compon. Lett.*, vol. 24, no. 8, pp. 518–520, Aug. 2014.

[30] A. Patrovsky, M. Daigle, and K. Wu, "Coupling mechanism in hybrid SIW–CPW forward couplers for millimeter-wave substrate integrated circuits," *IEEE Trans. Microw. Theory Techn.*, vol. 56, no. 11, pp. 2594–2600, Nov. 2008.

[31] Y. J. Cheng, W. Hong, K. Wu, and Y. Fan, "A hybrid guided-wave structure of half mode substrate integrated waveguide and conductor-backed slotline and its application in directional couplers," *IEEE Microw. Wireless Compon. Lett.*, vol. 21, no. 2, pp. 65–67, Feb. 2011.

[32] Z.-C. Hao, W. Hong, J.-X. Chen, X.-P. Chen, and K. Wu, "Compact super-wide bandpass substrate integrated waveguide (SIW) filters," *IEEE Trans. Microw. Theory Techn.*, vol. 53, no. 9, pp. 2968–2977, Sep. 2005.

[33] F. Mira, J. Mateu, S. Cogollos, and V. E. Boria, "Design of ultra-wideband substrate integrated waveguide (SIW) filters in zigzag topology," *IEEE Microw. Wireless Compon. Lett.*, vol. 19, no. 5, pp. 281–283, May 2009.

[34] R. S. Chen, S.-W. Wong, L. Zhu, and Q.-X. Chu, "Wideband bandpass filter using U-slotted substrate integrated waveguide (SIW) cavities," *IEEE Microw. Wireless Compon. Lett.*, vol. 25, no. 1, pp. 1–3, Jan. 2015.

[35] L. Huang, H. Cha, and Y. Li, "Compact wideband ridge half-mode substrate integrated waveguide filters," *IEEE Trans. Microw. Theory Techn.*, vol. 64, no. 11, pp. 3568–3579, Nov. 2016.

Dong-Fang Guan was born in Henan, China, in 1988. He received the B.S. and Ph.D. degrees from the College of Communications Engineering, PLA University of Science and Technology, Nanjing, China, in 2011 and 2016, respectively.

He is currently a Lecturer with the College of Electronic Science and Engineering, National University of Defense Technology, Changsha, China. His current research interests include microstrip antennas, array antenna, SIW technology, spoof surface plasmons, and metamaterials.

Peng You was born in Jiangxi, China. He received the B.S., M.S., and Ph.D. degrees in electrical engineering from the National University of Defense Technology (NUDT), Changsha, China, in 2005, 2008, and 2014, respectively.

Since 2014, he has been a Lecturer with the School of Electronic Science and Engineering, NUDT. His current research interests include the design of architecture for space information network and cognitive radar.

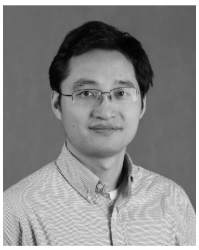

Qingfeng Zhang (S'07–M'11–SM'15) received the B.E. degree in electrical engineering from the University of Science and Technology of China, Hefei, China, in 2007, and the Ph.D. degree in electrical engineering from Nanyang Technological University, Singapore, in 2011.

From 2011 to 2013, he was with the Poly-Grames Research Center, Ecole Polytechnique de Montreal, Montreal, OC, Canada, as a Post-Doctoral Fellow. Since 2013, he has been with the Southern University of Science and Technology, Shenzhen, China, as an Assistant Professor. He has authored or co-authored more than 100 research papers. His current research interests include emerging novel electromagnetics technologies and multidisplininary topics.

Dr. Zhang was awarded Shenzhen Overseas High-Caliber Personnel in 2014, Guangdong Natural Science Funds for Distinguished Young Scholar in 2015, Shenzhen Nanshan Piloting Talents in 2016, and Guangdong Special Support Program for Top-Notch Young Talents in 2017. He has been served as an Associate Editor of IEEE ACCESS since 2017 and as a Lead Guest Editor of the *International Journal Antennas and Propagation* from 2014 to 2015. He was the publication chair of the IEEE ICCS in 2016 and a TPC member of several international conferences including EUCAP 2015, APCAP 2015, and EUCAP 2017. He serves on the Review Board of several microwave journals.

Ke Xiao was born in Hunan, China, in 1981. He received the B.S., M.S., and Ph.D. degrees from the College of Electronic Science and Engineering, National University of Defense Technology (NUDT), Changsha, China, in 2003, 2005, and 2011, respectively.

From 2008 to 2010, he was an Exchange Student with the Department of Electrical and Computer Engineering, National University of Singapore, Singapore. He is currently a Lecturer with the Department of Electronics Science and Technology, NUDT. His current research interests include computational electromagnetic, wideband antenna design, and metamaterials.

Shao-Wei Yong was born in Chongqing, China, in 1965. He received the B.S. degree in electrical engineering from the College of Communications Engineering, Nanjing, China, in 1986, and the M.S. and Ph.D. degrees in electrical engineering from the National University of Defense Technology, Changsha, China, in 1989 and 1997, respectively.

He is currently a Professor with the College of Electronic Science and Engineering, National University of Defense Technology. His current research interests include space information network and satellite communication.